Indian Geotechnical Journal, 39(1), 2009, 64-80

One-Dimensional Non-Reactive Contaminant Transport with Scale-Dependent Dispersion

E. C. Nirmala Peter[*], M. R. Madhav[**] and E. Saibaba Reddy[***]

Introduction

Determination of scale-dependent hydraulic and transport parameters of soils is essential for quantifying fluid flow and chemical transport through the subsurface. One of the key parameters used in the transport of the contaminant species is hydrodynamic dispersion coefficient. Several studies have shown that the dispersion coefficient increases with distance or travel time (Sposito *et al.*, 1986). From the experiments conducted on leaching columns, Yong and Warith (1989) suggested the variable nature of the dispersion coefficient and obtained a linear relationship between the dispersion coefficient (D_x) and the mean velocity (V_x). Watson *et al.* (2002) also indicated that the hydrodynamic dispersion coefficient was a non-linear function of the seepage velocity. Wang *et al.* (1998) suggested that the contaminant transport could be modeled accurately only if dispersion coefficient is allowed to increase with or adjusted to scale. Their study also indicated that the true migration or seepage velocity of the contaminant may not be obtained from Darcy's velocity divided by n (v/n where v – Darcy's velocity and n is the porosity of the porous medium). They observed that a close fit to the experimental data can be obtained by using the value of measured seepage velocity, V_x, defined as the velocity of the mean point ($C/C_0 = 0.5$) of the experimental break-through curve (Rumer, 1962), in the mathematical model. All these studies stressed on the variable nature of dispersion coefficient with scale and type of soil.

The Convection-Dispersion Equation (CDE) in general, has been in use for describing contaminant transport through the porous media. In the classical CDE, the dispersion coefficient is assumed constant, but the results from several field studies (Taylor and Howard, 1987, Domenico and Robbins, 1984, Toride et al., 1995) indicated scale-dependent dispersion i.e. dispersion coefficient increases with distance 'x' from the source of pollution. Many analytical solutions have been developed for CDE with scale-dependent dispersion e.g. Khan and Jury (1990), Pachepsky et al. (2000), Pang and Hunt (2001). These solutions are difficult to implement due to their highly idealized boundary conditions and parameters. As an alternative, numerical methods are often preferred as these methods are easier to implement than the analytical

* Assoc. Prof. in Civil Engg., J.N.T.U. College of Engg., Kukatpally, Hyderabad – 500 072, India. e-mail: ecnps@yahoo.co.uk

** Prof. of Emeritus, J.N.T.U. College of Engg., Kukatpally, Hyderabad –500 072, India. e-mail: madhav@iitk.ac.in

*** Prof. in Civil Engg., J.N.T.University, Kukatpally, Hyderabad –500 072, India. e-mail: sbreddy@yahoo.co.in

solutions. Mishra and Parker (1990) applied a hyperbolic distance-dependent dispersivity in a study on solute transport through porous media.

This paper presents the development of a numerical model for one-dimensional flow and dispersion considering power law variation of dispersion coefficient, D_x, with distance of contaminant travel as $D_x = D_d + mx^n$ where D_d - coefficient of diffusion, x - distance of contaminant travel, 'm' and 'n' are parameters which are dependent on the type of soil. In the present study, convective-dispersive transport for only non-reactive contaminant has been considered for deriving the governing equation. The partial differential equation is solved by the finite difference method. The solutions obtained from the proposed model are compared with the published long column experimental data of Huang *et al*. (1995).

Theory

Problem Definition

A view of the landfill (Figure 1(a)) indicating the different components is the basis for the numerical as well as the laboratory experimentation of the study of the scale-dependent dispersion. A simple schematic of the problem (Figure 1 (b)) shows a landfill resting on a low permeable soil layer of finite depth, overlying highly permeable strata. The concentration of the contaminant, C, at the base of the landfill is C_0 at any time greater than zero. The contaminant disperses through the low permeable layer into the next layer. The flow through the low permeable layer is considered as one-dimensional.

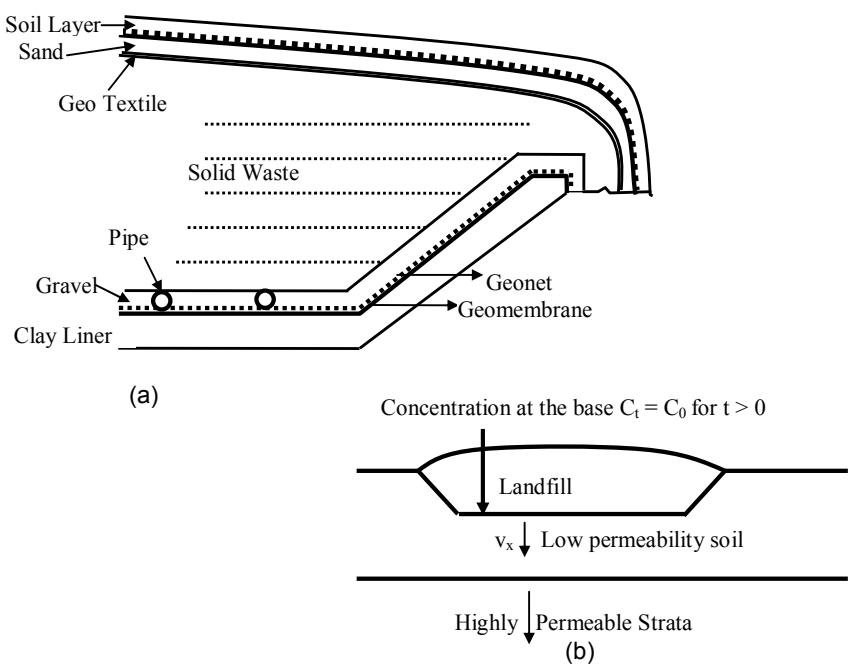

Fig. 1 (a) Schematic of Landfill Components and (b) Problem Description

For conceptualization of the model, the assumptions made are:

- One-Dimensional flow and dispersion through the low permeable strata.
- The source of contamination is continuous with the same concentration, C_0.
- The depth of the porous medium under consideration is finite.
- The porous medium is saturated.
- The hydrodynamic dispersion coefficient varies with distance.
- The concentration of the contaminant initially in the soil is zero.

Initial and Boundary Conditions

Landfills are of finite extent and have limited active life. If the landfill is constructed on low permeable soil, the time to reach peak concentration of any chemical is often small compared with the time scale imposed by the slow pollutant migration through the soil layer. In many practical situations the most hazardous pollutant has a maximum concentration, C_0, initially (zero time). This concentration will then decrease with time as leachate is transmitted through the soil. However if the height of the leachate in the landfill is large, then the concentration remains more or less constant. Though this assumption of constant concentration is extremely conservative, it is used because it covers many important aspects of the problem of pollutant migration through a finite layer. Therefore it is assumed that

$$C(x, 0) = 0 \text{ at } t = 0 \tag{1}$$

$$C(0, t) = C_0 \text{ for } t > 0 \tag{2}$$

The concentration in the underlying more permeable stratum will tend to zero if the base velocity is sufficiently large to remove the discharged leachate. However, in many cases the velocity being relatively small and also to provide a means of estimating this concentration it is assumed that the concentration in the underlying permeable stratum does not vary in the vertical or horizontal directions. Therefore

$$C(L_1, t) = C(L, t) \text{ for } L_1 > L \tag{3}$$

where L is the total depth or thickness of the stratum.

Governing Equation

The governing equation for one-dimensional convective-advective transport for non-reactive contaminant with scale-dependent dispersion coefficient is

$$D_x \frac{\partial^2 C}{\partial x^2} - \left(\frac{\partial D_x}{\partial x} - V_x \right) \frac{\partial C}{\partial x} = \frac{\partial C}{\partial t} \tag{4}$$

Where D_x [L^2/T] is the dispersion coefficient, V_x [L/T] is the measured seepage velocity, C [M/L^2T^2] is the concentration of the contaminant, t [T] is time and x [L] is the distance of travel of the contaminant. Several studies (Khan and

Jury (1990), Huang (1991), Toride et al.(1995), Huang et al., 1995, Pachepsky et al., 2000) have shown that the dispersivity increases with depth. They also indicated a non-linear variation of dispersivity with depth or distance (Figure 2).

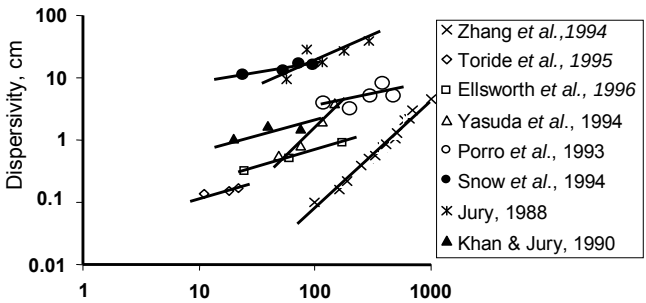

1.0

Fig. 2 Dependency of the Solute Dispersivity on Distance in Soils

In general dispersion coefficient, D_x is given by $D_x = \alpha v + D_d$ where α is the dispersivity, v – seepage velocity and D_d is the diffusion coefficient through the porous medium. However for a given contaminant and diffusion through a given porous medium, the coefficient of diffusion, D_d is constant. Therefore taking into consideration that the dispersion coefficient varies non-linearly with depth, a power law variation of the dispersion coefficient, $D_x = D_d + mx^n$ is considered. The governing equation is written as

$$(D_d + m.x^n)\frac{\partial^2 C}{\partial x^2} - (m.n.x^{n-1} - V_x)\frac{\partial C}{\partial x} = \frac{\partial C}{\partial t} \tag{5}$$

on normalizing equation (5) with X= x/L, T= t/t_0 and t_0= L/V_x, one gets

$$\left(\frac{D_d}{LV_x} + \frac{m.X^n L^{n-1}}{V_x}\right)\frac{\partial^2 C}{\partial X^2} - \left(\frac{m.n.X^{n-1}L^{n-1}}{V_x} - 1\right)\frac{\partial C}{\partial X} = \frac{\partial C}{\partial T} \tag{6}$$

On substituting $\frac{D_d}{LV_x} = \alpha_D$ and $\frac{m.L^{n-1}}{V_x} = \beta$ Eq. (6) transforms to

$$(\alpha_D + \beta.X^n)\frac{\partial^2 C}{\partial X^2} - (n.X^{n-1}\beta - 1)\frac{\partial C}{\partial X} = \frac{\partial C}{\partial T} \tag{7}$$

The initial and boundary conditions are given in Eqs. 1, 2 & 3.

Finite Difference Method of Solution

The partial differential equation describing the flow and transport processes includes terms representing derivatives of continuous variables. The

total length of the column is divided in to 'n' number of segments (Figure 3). The nodes are located at the centre of each segment. The concentration of the contaminant in each segment at any given time 't' is represented as $C_{(i-1,\ t)}$, $C_{(i,\ t)}$, etc. up to $C_{(n,t)}$. An equation is written for each nodal point. Finite difference method approximates the derivative in the partial differential equations as difference quotients, both in space and time, with respect to the interval between those adjacent nodes.

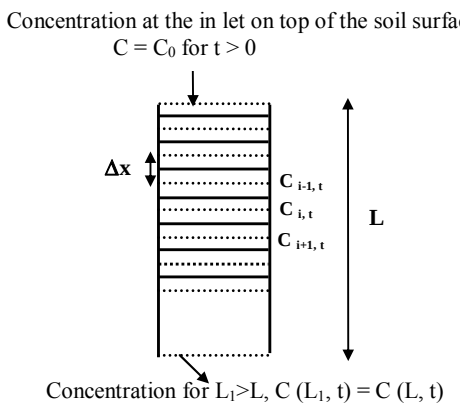

Fig. 3 Elements for Finite Difference

The first derivative of concentration, $\frac{\partial C}{\partial x}$ at a point midway between the nodes under consideration is given by the central difference formula as

$$\frac{\partial C}{\partial X} = \frac{(C_{i+1,t} - C_{i-1,t})}{2.\Delta X} \tag{8}$$

Similarly the second derivative is given by

$$\frac{\partial^2 C}{\partial X^2} = \frac{(C_{i+1,t} + 2.C_{i,t} - C_{i-1,t})}{(\Delta X)^2} \tag{9}$$

Substituting Eqs. (8) and (9) in the governing equation with scale-dependent dispersion with power law variation, Eq. (7) transforms to

$$(\alpha_D + \beta X^n)\left(\frac{(C_{i+1,t} + 2.C_{i,t} - C_{i-1,t})}{(\Delta X)^2}\right) - (n.X^{n-1}\beta - 1)\left(\frac{(C_{i+1,t} - C_{i-1,t})}{2.\Delta X}\right) = \left(\frac{(C_{i+1,t} - C_{i-1,t})}{\Delta T}\right) \tag{10}$$

The unknown concentration of the non-reactive contaminant is solved as

$$C_{i,t+\Delta t} = \left[\frac{(\alpha_D + \beta X^n).\Delta T}{(\Delta X)^2} + \frac{(n.X^{n-1}\beta - 1)}{2.\Delta x}.\Delta T\right].C_{i-1,t}$$

$$+\left(1 - 2.\frac{(\alpha_D + \beta X^n)}{(\Delta X)^2}.\Delta T\right).C_{i,t} + \left[\frac{(\alpha_D + \beta X^n).\Delta T}{(\Delta X)^2} - \frac{(n.X^{n-1}\beta - 1)}{2.\Delta X}.\Delta T\right].C_{i+1,t} \tag{11}$$

where

$\mu_x = \frac{(\alpha_D + \beta X^n).\Delta T}{(\Delta x)^2}$; $\beta_x = \frac{(n.X^{n-1}\beta - 1)}{2.\Delta x}.\Delta T$. On substitution of μ_x and β_x in Eq. (11), the above equation reduces to

$$C_{i,t+\Delta t} = [\mu_x + \beta_x].C_{i-1,t} + (1 - 2.\mu_x).C_{i,t} + [\mu_x - \beta_x].C_{i+1,t} \quad (12)$$

Check for Stability and Convergence

The stability and convergence of the solution is checked by evaluating the concentration of the contaminant at each of the nodes for different values of ΔT in Eq.11. The input parameters (Table 1) resulted in the Break-Through curves shown in Figure 4. The normalised time T is t/t_0. The Break-Through curves (BTC) are drawn for $\alpha_D = 1x10^{-5}$, $\beta = 0.1$, $n = 1.5$, $\Delta X = 0.02$, and for different values of ΔT equal to $1.5\ x10^{-3}$, $1\ x10^{-3}$, $9\ x10^{-4}$ and $7.5\ x10^{-4}$. The curves for all these values of ΔT converged to the same BTC. The values of ($\mu_x + \beta_x$), ($1 - 2\mu_x$) and ($\mu_x - \beta_x$) are positive for the above values of ΔT. However for ΔT equal to $2\ x10^{-3}$, the value of ($1 - 2\mu_x$) is negative while the other two values are positive. These values do not yield proper solution, and hence break-through curve couldn't be obtained. Therefore to obtain convergence of the curves, the size of the time step, ΔT should not exceed $1\ x10^{-3}$ for value of ΔX equal to 0.02. However it was also noted that the limiting value of ΔT changes with value of ΔX, e.g., for $\alpha_D = 1x10^{-5}$, $\beta = 0.1$, $n = 1.5$, $\Delta X = 0.01$, the limiting value of ΔT was $5x10^{-4}$. Thus each value of ΔX has a limiting value of ΔT for which the BTCs converge to a single curve.

Table 1 Input Parameters to Check the Stability of the Model for Different Values of ΔX and ΔT

Input Parameters	1	2	3	4	5	6	7
α_D	$1x10^{-5}$	$1x10^{-5}$	$1x10^{-5}$	$1x10^{-5}$	$1x10^{-5}$	$1x10^{-5}$	$1x10^{-5}$
β	0.1	0.1	0.1	0.1	0.1	0.1	0.1
n	1.5	1.5	1.5	1.5	1.5	1.5	1.5
ΔX	0.02	0.02	0.02	0.02	0.02	0.01	0.01
ΔT	$1x10^{-3}$	$1.5x10^{-3}$	$7.5x10^{-4}$	$9x10^{-4}$	$2x10^{-3}$	$4.5x10^{-4}$	$5x10^{-4}$
μ_x	0.250	0.3750	0.18751	0.22502	0.5	0.45004	0.50005
β_x	-0.021	-0.0319	-0.01594	-0.01913	-0.0425	-0.01913	-0.02125
$\mu_x + \beta_x$	0.229	0.3432	0.17158	0.20589	0.458	0.43092	0.4788
$1 - 2*\mu_x$	0.4999	0.2499	0624963	0.54995	$-1x10^{-4}$	0.09991	$-1x10^{-4}$
$\mu_x - \beta_x$	0.271	0.4069	0.20345	0.24414	0.543	0.46917	0.5213

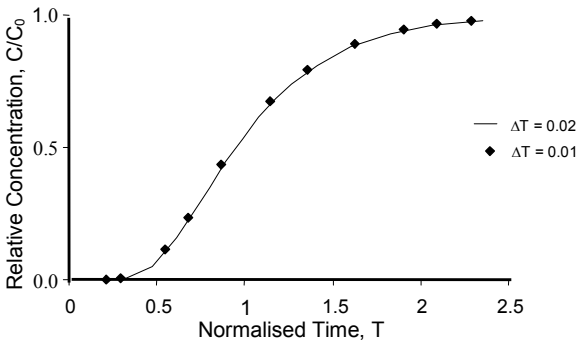

Fig. 4 Break-Through Curves for Different Values of ΔT

Parametric Study

The parameters α_D, β and n from Eq. (11) are identified as the key parameters that have the most influence on model calibration and predictions. In this study the input parameters and the ranges of these parameters within which they are varied must be justified. The analysis of the key parameters is performed so that a range of the "best" and "worst" scenarios could be simulated. The parameters α_D and β are given by

$$\alpha_D = \frac{D_d}{LV_x} \text{ and } \beta = \frac{mL^{n-1}}{V_x} \tag{13}$$

In the present study, NaCl solution is taken as the contaminant and the following values of D_d, L and V_x are assumed to obtain the maximum and minimum values of the parameters:

1. $D_d = 1.5 \times 10^{-6}$ cm^2/s [$D_d = W.D_0$]; D_0 ranges from 1.47×10^{-5} to 1.612×10^{-5} cm^2/s for a non-adsorbing species like NaCl; the value of 'W' ranges from 0.5 to 0.01. Therefore a D_d value of 1.50×10^{-5} cm^2/s and W value of 0.1 are assumed (Shackelford and Rowe, 1998).
2. In landfill construction, the thicknesses of the clay liner and other layers such as filters, etc., vary between 30 cm to a maximum of 200 cm. But for the present study, the range of L is taken from 1 cm to 200 cm.
3. The range of measured seepage velocity, V_x, keeping in view the different types of soils is between 1×10^{-2} and 1×10^{-9} cm/s.
4. A minimum value of $\alpha_{Dmin} = 7.5 \times 10^{-7}$, and a maximum value of α_{Dmax} = 1500 result from the above assumptions. However for the present study the values of α_D are varied from 1×10^{-7} to 100.
5. The key parameter is β (mL^{n-1}/V_x) which is dependent on L, V_x, m and n. The parameters 'm' and 'n' are dependent on the type of the soil. L and V_x are taken within the range mentioned above. The parametric study for the model is carried out considering a range of 'n' between 1 and 5, and that of β from 0.001 to 1 (Figures 5 through 10).

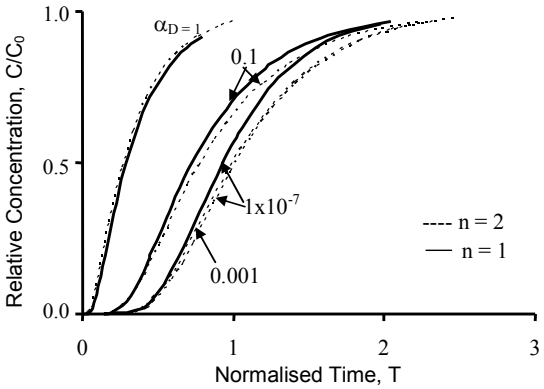

Fig. 5 Normalised Time vs. Relative Concentration for β = 0.1 and for Different Values of $\alpha_D \leq 1$ and n

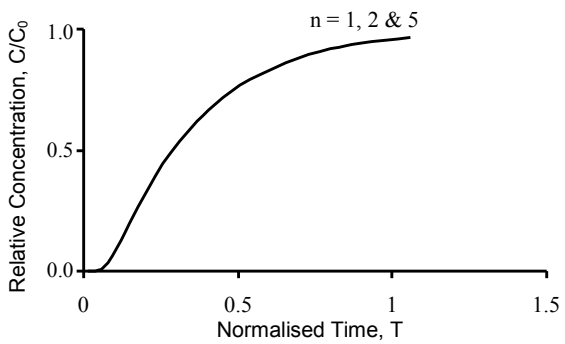

Fig. 6 Normalised Time vs. Relative Concentration for α_D = 1 and β = 0.1

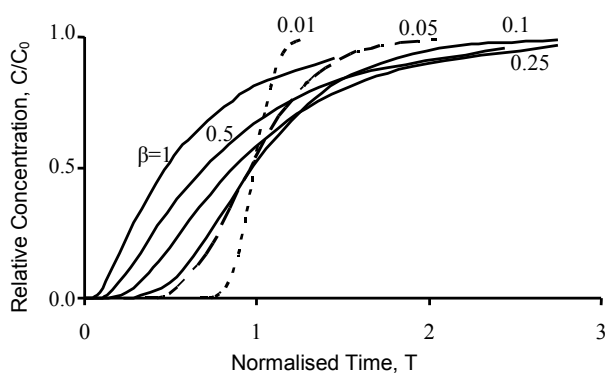

Fig. 7 Normalised Time vs. Relative Concentration for α_D = 1x10^{-7}, n= 1.5 and for Different Values of β

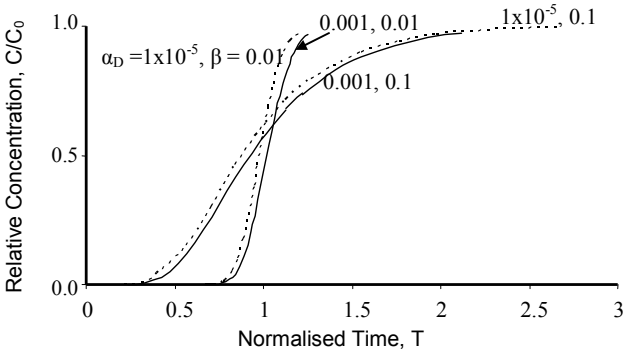

Fig. 8 Normalised Time vs. Relative Concentration for α_D = 1x10^{-5} & 0.001, β = 0.01 & 0.1 and n = 1

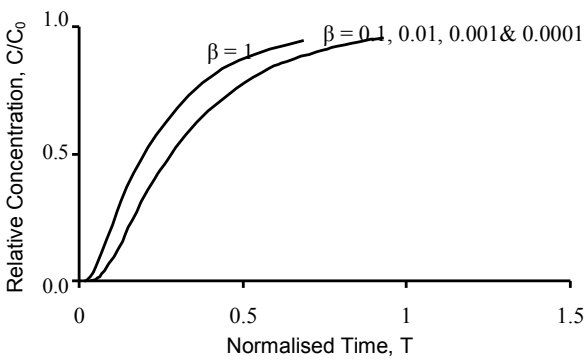

Fig. 9 Normalised Time vs. Relative Concentration for α_D = 1, n = 1.5

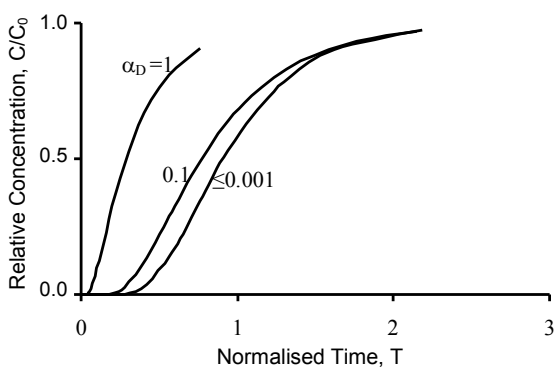

Fig. 10 Normalised Time vs. Relative Concentration for β= 0.1, n = 1

Discussion

The parametric study with the key parameters n, α_D (D_d/LV_x) and β (mL^{n-1}/V_x) yielded the following observations. For low values of α_D i.e., for 0.001 to$1x10^{-7}$, the effect of n on the break-through curves (Figure 5) is to increase the normalised time for increase in the value of 'n' from 1 to 2. The difference in the break-through curves (BTC) for n equal to 1 and 2 decreases for α_D increasing to 0.1 while for α_D = 1 the BTCs for values of n equal to 1, 2 and 5 converge to a single curve (Figure 6). Low values of α_D (≤ 0.001) indicate high seepage velocities greater than 10^{-3} cm/s through the soil. α_D value decreases further with increase in value of 'L'. Therefore the effect of 'n' on break-through curves is significant in coarse soils for velocities of flow greater than 10^{-3} cm/s. α_D increases with decrease in velocity resulting in decreasing the effect of 'n' on break-through curves. For soils with very low velocities (≤ 10^{-6} cm/s), the BTCs converge to a single curve indicating that in soils with low seepage velocity (clay) the effect of 'n' ceases because only diffusive process of contaminant transport exists in the soil. In soils with velocity between 10^{-2} to 10^{-4} cm/s, the normalised time value of the break-through curves increases slightly with increase in the 'n' value. For soils with velocity between 10^{-4} to 10^{-6} cm/s, the difference in BTCs for n = 1 and 2 decreases with decrease in seepage velocity i. e. increase in α_D.

Break-through curves could not be drawn for α_D < 0.001 and β < 0.01. For α_D < 0.001 and β < 0.01, the seepage velocity through 1 cm length of the soil is greater than 10^{-2} cm/s. As velocity increases above 10^{-2} cm/s, the flow becomes completely advective. Therefore break-through curves could not be obtained. Similarly for α_D ≥ 1 and β ≥ 0.1, the velocity is less than 10^{-6} cm/s and the contaminant transport becomes completely diffusive and the break-through curves converge to a single curve.

In soils with velocity between 10^{-3} to 10^{-6} cm/s, the break-through curves for any value of α_D ≤ 0.001 and β = 0.01 have the same range of T value of 0-1.1 for the variation of C/C_0 from 0 to 0.96. All these curves remain at zero relative concentration up to a T value of 0.65. C/C_0 increases rapidly to a value of 0.96 at about a T value of 1.1 (Figures 7 and 8). This indicates that the movement of solute particles in soils may not follow Brownian motion. The Levy motion can predict the BTCs (even with heavier tails) better than the Brownian motion. Particles undergoing Levy motion can be characterized as Brownian motion except for occasional large jumps. These jumps are clustered and in this type of motion, the particles trapped in relatively stagnant vortices for periods of time, travel within 'jets' of high velocity fluid (Weeks et al., 1995). This Levy motion explains the stagnant zero relative concentration up to T value of 0.65 and the rapid increase in the relative concentration to reach a value of 0.96 at about T=1.1. This response confirms that the Levy motion is predominant in soils with seepage velocity between 10^{-3} to 10^{-6} cm/s.

The range of V_x and m for various values of α_D and β are presented in Table 2. This study resulted in the following conclusions with reference to the effect of α_D, β and n on the predicted break-through curves.

Break-through curves cannot be obtained for α_D ≤ 0.001 and β < 0.01 due to advective transport of the contaminant.

Table 2 Range of V_x and m Corresponding to Different Values of α_D and β with n Equal to 1 and 2

S. No.	α_D	β	V_x (cm/s)	m
1	≤0.001	0.01	10^{-3}	10^{-6}-10^{-2}
2	0.001<α_D≤0.1	≤ 0.1 (0.1&0.01)	10^{-3}-10^{-6}	10^{-12}-10^{-6}
3	≥ 1	≥ 0.1	10^{-9}-10^{-7}	10^{-13}-10^{-8}
4	≥ 1	≤ 0.1	10^{-4}-10^{-8}	10^{-12}-10^{-7}
5	< 0.01	0.1	10^{-5}-10^{-7}	10^{-7}-10^{-11}

The normalised time (T) over which the relative concentration (C/C_0) varies from 0 to any specific value (ex. 0.96) increases with increase in the n value and decrease in the value of α_D (Figure 5). The parameter 'n' is effective only in the range of seepage velocities between 10^{-2} to 10^{-6} cm/s.

The break-through curves are not affected by the n value and converge to a single curve for any set of α_D and β for $\alpha_D \geq 1$ and $\beta \geq 0.1$ (Figure 6) due to diffusive transport of the contaminant.

The break-through curves for any value of $\alpha_D \leq 0.001$ and $\beta = 0.01$ have the same range of T values of approximately 0 to 1.1 for the variation of C/C_0 from 0.0 to 0.96. The relative concentration in all these curves remains at zero up to a T value of 0.65 and increases rapidly to obtain a value of 0.96 at about a T value of 1.1 (Figures 7 and 8). This shows the Levy motion of the contaminant through the porous medium with seepage velocities between 10^{-3} to 10^{-6} cm/s.

The BTCs converge to a single curve for a given values of $\alpha_D \geq 1$ and values of $\beta \leq 0.1$ (Figures 9).

The BTCs converge to a single curve for a given value of $\beta \geq 0.1$ and values of $\alpha_D < 0.01$ (Figures 7 and 10).

Verification of the Solution

Power Law Variation of Dispersion Coefficient with Experimental Data of Huang et al. (1995)

Laboratory tracer (NaCl) experiments are conducted to investigate solute transport in 12.5 m long, horizontally placed homogeneous sand column and break-through curves obtained. The concentration of the contaminant in the column is measured with electrical conductivity probes inserted at every 50 cm interval. The relative concentrations of the contaminant for various time periods at each of the locations (2 m, 5 m, 8 m and 11 m) are used as per the Figure 11 (Huang *et al*., 1995). The data of times and relative concentrations is furnished in Table 3.

Table 3 Experimental Data for Different Locations of the Homogeneous Column from Huang *et al.* (1995)

x = 2 m		x = 5 m		x = 8 m		x = 11 m	
Time (h)	C/C_0	Time (h)	C/C_0	Time (h)	C/C_0	Time (h)	C/C_0
4.810	0	12.282	0.0317	20.747	0.0714	30.871	0.2460
4.979	0.0159	12.614	0.0476	20.913	0.1269	31.701	0.3094
5.145	0.0476	12.946	0.0763	22.075	0.2539	32.697	0.4285
5.228	0.0952	13.278	0.1428	22.987	0.4047	33.527	0.5634
5.311	0.2142	13.444	0.2220	24.398	06348	34.522	0.7062
5.643	0.3490	13.610	0.3015	25.228	0.7855	35.601	0.8173
5.710	0.5633	13.942	0.3967	26.556	0.8967	37.012	0.9364
5.726	0.7380	14.274	0.4920	28.548	0.9839	39.004	0.9990
5.783	0.8094	14.439	0.6268	30.041	0.9990		
5.809	0.9120	14.770	0.7538				
6.307	0.9681	15.269	0.8810				
6.781	0.9998	15.601	0.9284				
		17.759	0.9980				

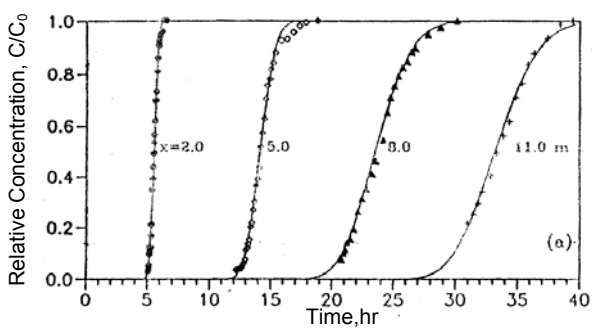

Fig. 11 Concentration Distribution in a Homogeneous Column (Huang et al. 1995)

Verification of the solution for power law variation of dispersion coefficient is carried out by developing break-through curves at different locations, i.e. at 2 m, 5 m, 8 m and 11 m, of the column. The seepage velocities calculated from the ratio of the distance of travel, L, (2 m, 5 m, 8 m and 11 m) to the time corresponding to a relative concentration of 0.5 ($t_{0.5}$) obtained from the Break-Through curves (BTC's) are used to predict the concentration profiles. Parameters m and n are obtained from log-log plot of distance vs. dispersion coefficient calculated from the formula (Fried, 1975)

$$D_x = (1/8)\ \{[(x - v_x\, t_{0.16})/\ (t_{0.16})^{0.5}] - [(x - v_x\, t_{0.84})/\ (t_{0.84})^{0.5}]\}^{\,2} \qquad (13)$$

Where $t_{0.16}$ and $t_{0.84}$ are the time periods which correspond to the relative concentrations of 0.16 and 0.84 respectively. Comparison of these numerical solutions and experimental data is presented in Figure 12. The input parameters for the numerical solutions are furnished in Table 4. The 'm' and 'n' values

obtained from the log-log plot of D_x (Fried, 1975) and distance, x, are 5.01×10^{-6} and 1.5946 respectively. However it is observed that the numerical solutions using these parameters deviated from the laboratory concentration profiles slightly. This may be due to the inaccuracies involved in the measurement or interpolation of the relative concentrations from the Figure 11 and also because of using Fried's analytical solution for the calculation of D_x. The model was calibrated to obtain solutions with values of 'm' equal to 5.01×10^{-6}, 2.9×10^{-6}, 2.15×10^{-6} and 2×10^{-6}, and an 'n' value of 1.5635 for 2 m, 5 m, 8 m, and 11 m lengths of the column respectively, which fitted well with the experimental data, Figure 12.

Table 4 Input Parameters for Break-through Curves at Different Locations of the Homogeneous Column

Depth, x	2 m	5 m	8 m	11 m
D_d (cm^2/s)	1.5×10^{-6}	1.5×10^{-6}	1.5×10^{-6}	1.5×10^{-6}
m	4.85×10^{-6}	2.9×10^{-6}	2.15×10^{-6}	2×10^{-6}
n	1.5635	1.5635	1.5635	1.5635
L (cm)	200	500	800	1100
V_x(cm/s)	0.009921	0.0098	0.009416	0.0092
α_D	7.56×10^{-6}	3.06×10^{-7}	1.99×10^{-7}	1.48×10^{-7}
β	0.009678	0.009819	0.009873	0.01125

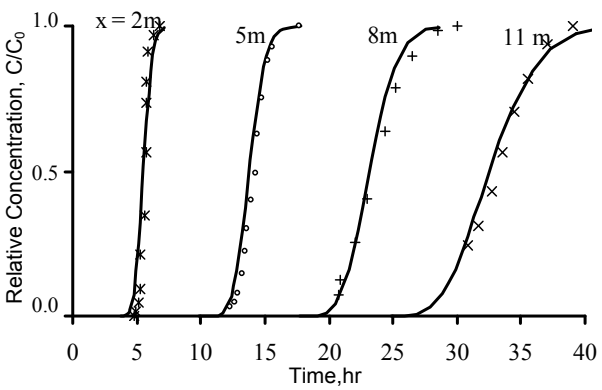

Fig. 12 Comparison of the Numerical Solutions with Experimental Data of Huang *et al.*, (1995)

Comparison of Scale-Dependent Dispersion Model with the Classical Constant Dispersion Model

Laboratory column test is conducted on 94 cm soil column using experimental set up (Figure 13) to study the scale effect of dispersion coefficient. The NaCl contaminant samples are collected at 14 cm, 34 cm, 54 cm, 74 cm and 94 cm of the column from the top of the soil surface. The dispersion coefficients for each depth are calculated from Fried's analytical

solution (Eq.13). Parameters 'm' and 'n' are obtained from the log-log plot of depth of column vs. dispersion coefficients. The seepage velocities from evaluated from the break-through curves were used to predict the break-through curves for both classical convection-dispersion model which assumes constant dispersion coefficient and the scale-dependent dispersion model with power law variation of dispersion coefficient with distance. These numerical curves are compared with the measured data at respective depths. This study indicated that the model considering constant dispersion coefficient over predicts the measured data while the proposed model with power law variation of dispersion coefficient yields BTCs which compare well with the measured data (Figures 14 & 15).

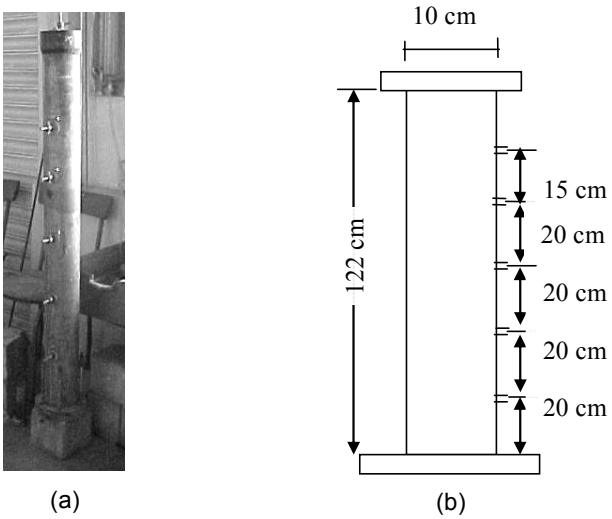

Fig. 13 Experimental Set-Up (a) Photograph of the Mould (b) Schematic Diagram of the Mould

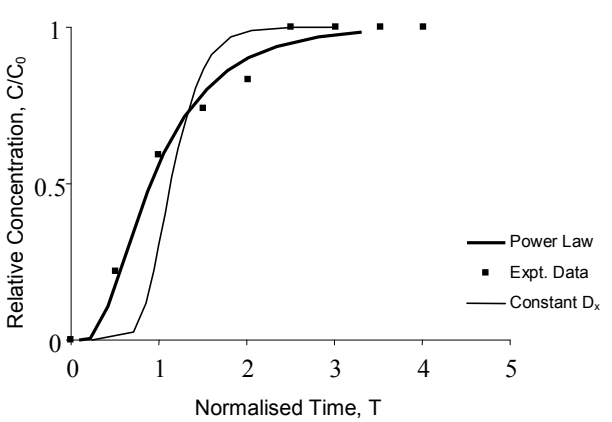

Fig.14 Break-through Curves at 34 cm Depth of the Column

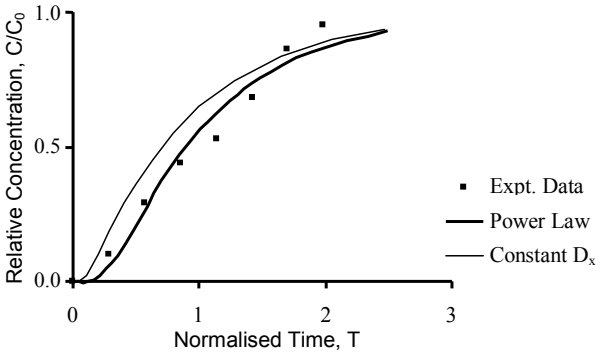

Fig.15 Break-through Curves at 94 cm Depth of the Column

Conclusions

A numerical solution is developed for the governing equation with a variable dispersion coefficient for one-dimensional non-reactive contaminant transport, with convection and dispersion as processes of transport. The dispersion coefficient is assumed to vary as a power law function of distance. This solution predicts the concentrations of the contaminant at all locations satisfactorily for the column and the results are in good agreement with the experimentally measured concentration data while the solution to classical convection-dispersion equation over predicts the concentration profiles. It is also observed that the use of measured seepage velocity (v_m) from break-through curves in the mathematical model achieved a close fit to the experimental data. This study establishes that dispersion coefficient essentially varies as a power function with distance over the scale of the experiment or measurement. The proposed model predicts the concentration profiles accurately for non-reactive contaminants where as the model with constant dispersion over predicts the concentration profiles.

List of Notations

ΔT	Normalised time increment
ΔX	Ratio of the distance between the centres of two successive segments to the total length of the column
BTC	Break-through curve
C_0	The concentration of the contaminant Introduced as a continuous source
CDE	Convection-dispersion equation
C_{it}	Concentration of the contaminant at the centre of the i^{th} segment at any time 't'

$C_{it+\Delta t}$	Concentration of the contaminant at the centre of the i^{th} segment at time '$t+\Delta t$'
D	Dispersion coefficient
D_d	Coefficient of diffusion in porous medium
D_x	Dispersion coefficient in the direction of flow in one-dimensional contaminant transport through a soil column
m	A multiplying factor which is dependent on the type of soil, and used in the expressions for the variable dispersion coefficient
n	Exponent used in the power law variation of the dispersion coefficient and dependent on the type of soil
T	Normalised time, t/t_0 where t_0 is L/V_x
V_x	Measured seepage velocity for the soil column
x	Distance in cm from the top surface of the column (source) to the point at which measurement of the concentration of the contaminant was taken

References

Domenico, P. A., and Robbins, G. A. (1984): 'A dispersion scale effect in model calibrations and field tracer experiments', *J. Hydrology*, 70:pp.123-132.

Fried, J. J. (1975): *Ground Water Pollution*, Elsevier Scientific Publishing Company, Amsterdam – Oxford, New York.

Huang, K., Toride, N., van Genuchten, M. Th.(1995): 'Experimental investigation of solute transport in large, homogeneous and heterogeneous, saturated soil columns', *Transport in porous media*, 18: pp.283-302.

Khan, A. U. H., and Jury, W. A. (1990): 'A laboratory study of the dispersion scale effect in column outflow experiments', *J. Contaminant Hydrology* 5, pp.19-131.

Mishra S., Parker J.C. (1990): 'Analysis of solute transport with a hyperbolic scale-dependent dispersion model', *Hydrol. Proc*. 4: pp.45-70.

Pachepsky, Y., David Benson, and Walter Rawls (2000): 'Simulating scale-dependent solute transport in soils with the Fractional advective-dispersive equation', *Soil Sci. Soc. Am. J*. 64: pp.1234-1243.

Pang, L., and Hunt, B. (2001): 'Solutions and verification of a scale-dependent dispersion model', *Journal of Contaminant Hydrology*, 53(1-2), pp. 21-39.

Rumer, R. R. (1962): 'Longitudinal dispersion in steady and unsteady flow', *Journal of the Hydraulic Division*, ASCE, HY4, pp. 147-172.

Sposito, G., White, R. E., Darrah, P. R., and Jury, W. A., (1986): 'A transfer function model of solute transport through soil, the convection-dispersion equation', *Water Resour. Res*. 22, pp. 255-262.

Taylor, S. R., and Howard, K. W. F. (1987): 'A field study of scale-dependent dispersion in a sandy aquifer', *Journal of Hydrology,* 90, pp.11-17.

Toride, N., Leij, F., and van Genuchten, M. Th. (1995): 'The CXTFIT code for estimating transport parameters from laboratory or field tracer experiments. Version 2', *Research Report 137*, US Salinity Lab., Riverside, CA.

Wang, J. C., Booker, J. R., Carter, J. P. (1998): 'Experimental investigation of contaminant transport in porous media', *Research Report No. R776*, Centre for Geotechnical Engineering, Department of Civil Engineering, The University of Sydney.

Watson, S. J., Barry, D. A., Schotting, R. J., Hassanizadeh, S. M. (2002): 'Validation of classical density-dependent solute transport theory for stable high-concentration-gradient brine displacements in coarse and medium sands', *Advances in Water Resources* 25, 99.611-635

Yong, R. N., and Warith, M. A. (1989): 'Contaminant migration effect on dispersion coefficient', *ASTM*, STP 1095, pp. 69-80.